

Raman response of magnetic excitations in cuprate ladders and planes

K. P. Schmidt*

Institut für Theoretische Physik, Universität zu Köln, Zùlpicher Strasse 77, D-50937 Köln, Germany

A. Gössling

II. Physikalisches Institut, Universität zu Köln, Zùlpicher Strasse 77, D-50937 Köln, Germany

U. Kuhlmann and C. Thomsen

Institut für Festkörperphysik, Technische Universität Berlin, Hardenbergstrasse 36, D-10623 Berlin, Germany

A. Löffert, C. Gross, and W. Assmus

Physikalisches Institut, J.W. Goethe-Universität, Robert-Mayer-Strasse 2-4, D-60054 Frankfurt a. M., Germany

(Received 22 March 2005; revised manuscript received 15 July 2005; published 15 September 2005)

A unified picture for the Raman response of magnetic excitations in cuprate spin-ladder compounds is obtained by comparing calculated two-triplon Raman line shapes to those of the prototypical compounds SrCu_2O_3 (Sr123), $\text{Sr}_{14}\text{Cu}_{24}\text{O}_{41}$ (Sr14), and $\text{La}_6\text{Ca}_8\text{Cu}_{24}\text{O}_{41}$ (La6Ca8). The theoretical model for the two-leg ladder contains Heisenberg exchange couplings J_{\parallel} and J_{\perp} plus an additional four-spin interaction J_{cyc} . Within this model Sr123 and Sr14 can be described by $x := J_{\parallel}/J_{\perp} = 1.5$, $x_{\text{cyc}} := J_{\text{cyc}}/J_{\perp} = 0.2$, $J_{\perp}^{\text{Sr123}} = 1130 \text{ cm}^{-1}$ and $J_{\perp}^{\text{Sr14}} = 1080 \text{ cm}^{-1}$. The couplings found for La6Ca8 are $x = 1.2$, $x_{\text{cyc}} = 0.2$, and $J_{\perp}^{\text{La6Ca8}} = 1130 \text{ cm}^{-1}$. The unexpected sharp two-triplon peak in the ladder materials compared to the undoped two-dimensional cuprates can be traced back to the anisotropy of the magnetic exchange in rung and leg direction. With the results obtained for the isotropic ladder, we calculate the Raman line shape of a two-dimensional square lattice using a toy model consisting of a vertical and a horizontal ladder. A direct comparison of these results with Raman experiments for the two-dimensional cuprates R_5CuO_4 ($\text{R}=\text{La}, \text{Nd}$), $\text{Sr}_2\text{CuO}_2\text{Cl}_2$, and $\text{YBa}_2\text{Cu}_3\text{O}_{6+\delta}$ yields a good agreement for the dominating two-triplon peak. We conclude that short-range quantum fluctuations are dominating the magnetic Raman response in both ladders and planes. We discuss possible scenarios responsible for the high-energy spectral weight of the Raman line shape, i.e., phonons, the triple-resonance, and multiparticle contributions.

DOI: [10.1103/PhysRevB.72.094419](https://doi.org/10.1103/PhysRevB.72.094419)

PACS number(s): 75.40.Gb, 75.50.Ee, 75.10.Jm

I. INTRODUCTION

Strongly correlated electron systems in low dimensions are of fundamental interest because of their fascinating properties resulting from strong quantum fluctuations.¹⁻³ Especially in the case of the high- T_c cuprate superconductors, the role of quantum fluctuations is heavily debated. Two-magnon Raman scattering has been proven to be a powerful tool to study quantum fluctuations in the magnetic sector.⁴⁻⁹ In contrast to the well-understood magnon dispersion as measured by inelastic neutron scattering,¹⁰⁻¹⁴ the quantitative understanding of the two-magnon line shape in the Raman response^{5,6} and in the optical conductivity¹⁵⁻¹⁸ remains an issue open to debate.

Interestingly, in the so-called cuprate ladder systems like Sr123 or the telephone-number compounds $(\text{Sr}, \text{Ca}, \text{La})_{14}\text{Cu}_{24}\text{O}_{41}$, a prominent peak in the magnetic Raman response is observed at the same energy of $\sim 3000 \text{ cm}^{-1}$, as in the two-dimensional (2D) compounds.^{19,20,22,23} In contrast to the gapless long-range-ordered two-dimensional compound, the quasi-one-dimensional two-leg ladders are known to be realizations of a gapped spin liquid.²¹ Because the elementary excitations above this ground state are triplons,²⁴ we call the corresponding Raman response as two-triplon Raman scattering.

On the one hand, one may expect that the Raman response is dominated by short-range, high-energy excitations, suggesting a certain similarity between ladders and planes, both being built from edge-sharing Cu_4 plaquettes. The peak frequencies are, in fact, at 3000 cm^{-1} . On the other hand, the line shape and, in particular, the peak width strongly varies between different compounds. In 2D, the peak width is of the order of 1000 cm^{-1} , in La6Ca8 $\sim 500 \text{ cm}^{-1}$, in Sr123 and Sr14 only $100\text{--}200 \text{ cm}^{-1}$. Because of the observation of a very sharp two-triplon Raman line in the spin liquid Sr14, Gozar *et al.* have questioned whether the large linewidth in 2D and the related, heavily discussed spectral weight above the two-magnon peak can be attributed to quantum fluctuations.²⁰

In the last few years, theoretical developments in the field of quasi-one-dimensional systems, namely, the quantitative calculation of spectral densities,²⁵⁻³¹ has led to a deeper understanding of magnetic contributions to the Raman response of undoped cuprate ladders. Besides the usual Heisenberg exchange terms, the minimal magnetic model includes four-spin interactions that are four to five times smaller than the leading Heisenberg couplings.^{19,27,28,32,33} The existence and the size of the four-spin interactions are consistent with theoretical derivations of generalized t - J models from one-band or three-band Hubbard models.³⁴⁻⁴⁰

In the present paper we show that the strong variation of the linewidth can be traced back to changes of the spatial anisotropy of the exchange constants. The sharp Raman line in Sr14 and Sr123 results from $x=1.5$, the increased linewidth in La6Ca8 reflects $x=1.2$, and the isotropic coupling $x=1$ for the square lattice yields the much larger width observed in 2D. In fact, we obtain a quantitative description of the dominant Raman peak in 2D using a toy model that mimics the 2D square lattice by the superposition of a vertical and a horizontal ladder. We thus conclude that the dominant Raman peak is well described by short-range excitations.

Besides the dominant two-triplon peak, the large spectral weight measured at high energies remains an open problem for the cuprate ladders and planes. We review possible sources of the high-energy spectral weight that were suggested in the past, e.g., quantum fluctuations,^{26,41–45} the role of spin-phonon interaction,^{4,46–51} and the triple resonance.^{5,52–54} In case of the cuprate planes, no final conclusion concerning the origin of the high-energy weight can be drawn; but in the case of the cuprate ladders, the spin-phonon coupling and the triple resonance can be ruled out.

II. MODEL

In Raman scattering, multiparticle excitations with zero change of the total spin can be measured. Starting at $T=0$ from a $S=0$ ground state, the singlet excitations with combined zero momentum are probed. The Raman response in spin ladders has been calculated by first-order perturbation theory⁵⁵ and by exact diagonalization.⁵⁶ In this work, Raman line shapes are presented, obtained from continuous unitary transformations (CUT) using rung triplons as elementary excitations.^{26,32} The results are not resolution limited because neither finite-size effects occur nor an artificial broadening is necessary.

For zero hole doping, the minimum model for the magnetic properties of the $S=1/2$ two-leg ladders is an antiferromagnetic Heisenberg Hamiltonian plus a cyclic four-spin exchange term H_{cyc} ^{27,57,58}

$$H = J_{\perp} \sum_i \mathbf{S}_{1,i} \mathbf{S}_{2,i} + J_{\parallel} \sum_{i,\tau} \mathbf{S}_{\tau,i} \mathbf{S}_{\tau,i+1} + H_{\text{cyc}} \quad (1a)$$

$$H_{\text{cyc}} = J_{\text{cyc}} \sum_i K_{(1,i),(2,i),(2,i+1),(1,i+1)} \quad (1b)$$

$$\begin{aligned} K_{(1,1),(1,2),(2,2),(2,1)} \\ = K_{1234} = (\mathbf{S}_1 \mathbf{S}_2)(\mathbf{S}_3 \mathbf{S}_4) + (\mathbf{S}_1 \mathbf{S}_4)(\mathbf{S}_2 \mathbf{S}_3) - (\mathbf{S}_1 \mathbf{S}_3)(\mathbf{S}_2 \mathbf{S}_4), \end{aligned} \quad (1c)$$

where i denotes the rungs and $\tau \in \{1, 2\}$ the legs. The exchange couplings along the rungs and along the legs are denoted by J_{\perp} and J_{\parallel} , respectively. The relevant couplings modeling Sr123 and Sr14^{59,60} are illustrated in Fig. 1. There is also another way to include the leading four-spin exchange term by cyclic permutations,^{27,33} which differs in certain two-spin terms from Eq. (1).³³ Both Hamiltonians are iden-

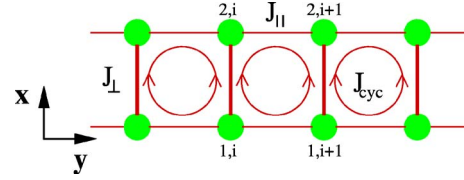


FIG. 1. (Color online) Schematic view of a two-leg ladder [notation as in Eq. (1)]. The circles denote the positions of Cu^{2+} ions carrying a spin $\frac{1}{2}$ each. The crystallographic axes are such that $x \parallel b$ and $y \parallel a$ for Sr123 and $x \parallel a$ and $y \parallel c$ for Sr14.

tical except for couplings along the diagonals if J_{\perp} and J_{\parallel} are suitably redefined.⁶¹

At $T=0$ the Raman response $I(\omega)$ is given by the retarded resolvent

$$I(\omega) = -\frac{1}{\pi} \text{Im} \langle 0 | \mathcal{O}^\dagger (\omega - H + i\delta)^{-1} \mathcal{O} | 0 \rangle. \quad (2)$$

The observables $\mathcal{O}^{\text{rung}}$ (\mathcal{O}^{leg}) for magnetic light scattering in rung-rung (leg-leg) polarization read in leading order^{62,63}

$$\mathcal{O}^{\text{leg}} = A_0^{\text{leg}} \sum_i (\mathbf{S}_{1,i} \mathbf{S}_{1,i+1} + \mathbf{S}_{2,i} \mathbf{S}_{2,i+1}) \quad (3a)$$

$$\mathcal{O}^{\text{rung}} = A_0^{\text{rung}} \sum_i \mathbf{S}_{1,i} \mathbf{S}_{2,i}. \quad (3b)$$

The factors A_0^{leg} and A_0^{rung} depend on the underlying microscopic electronic model. It is beyond the scope of the present work to compute them. The results will be given in units of these factors squared. In this paper, we will only consider nonresonant Raman excitation processes. We discuss which laser energy should be used in order to investigate the nonresonant regime.

III. METHOD

Technically, we employ a CUT to map the Hamiltonian H to an effective Hamiltonian H_{eff} , which conserves the number of rung-triplons, i.e., $[H_0, H_{\text{eff}}] = 0$ where $H_0 := H|_{\{J_{\parallel}=0; J_{\text{cyc}}=0\}}$.^{64–66} The ground state of H_{eff} is the rung-triplon vacuum. For the response function $I(\omega)$, the observable \mathcal{O} is mapped to an effective observable \mathcal{O}_{eff} by the same CUT. The CUT is implemented in a perturbative fashion in $x = J_{\parallel}/J_{\perp}$ and $x_{\text{cyc}} = J_{\text{cyc}}/J_{\perp}$. The effective Hamiltonian is calculated up to high orders (1-triplon terms: 11th, two-triplon terms: 10th order). The effective observable \mathcal{O}_{eff} is computed to order 10 in the two-triplon sector.

The resulting plain series are represented in terms of the variable $1 - \Delta^{\text{SG}}/(J_{\parallel} + J_{\perp})$ ^{67,68} where Δ^{SG} is the one-triplon gap. Then standard Padé extrapolants⁶⁹ yield reliable results up to $J_{\parallel}/J_{\perp} = 1 - 1.5$ depending on the value of J_{cyc}/J_{\perp} . Consistency checks were carried out by extrapolating the involved quantities before and after Fourier transforms. In case of inconclusive extrapolants, the bare truncated series are used. We will estimate the overall accuracy below by comparing to density matrix renormalization group (DMRG) results.²⁷ The Raman line shape is finally calculated as a

continued fraction by tridiagonalization of the effective two-triplon Hamiltonian.

Sectors with an odd number of triplons are inaccessible by Raman scattering because of the invariance of the two observables $\mathcal{O}_{\text{eff}}^{\text{leg}}$ and $\mathcal{O}_{\text{eff}}^{\text{rung}}$ with respect to reflections about the centerline of the ladder.²⁶ Thus, only excitations with an even number of triplons matter. Therefore, the leading contributions to the Raman response come from the two-triplon sector. It was shown earlier that the two-triplon contribution is the dominant part of the Raman response at low and intermediate energies.^{26,70} The role of the four-triplon contribution for the high-energy spectral weight will be discussed at the end of this work.

IV. CUPRATE LADDERS

In this part we will compare the theoretically obtained two-triplon contributions to the experimental line shapes of the cuprate ladders Sr123 and Sr14. The crystals of Sr123 have been grown and measured under the same conditions as described in Refs. 71 and 19 while the data of Sr14 have been provided by Gozar *et al.*²⁰ The experimental Raman line shape depends strongly on the laser energy because resonant contributions are present. This becomes apparent in a strong anisotropy between the width of the two-triplon peak in leg and rung polarization for laser energies $\omega_{\text{exc}} = 2-3$ eV. The width of the two-triplon peak in leg polarization is much sharper. For laser energies $\omega_{\text{exc}} < 2$ eV, the strong anisotropy between both polarizations vanishes.²⁰ It is therefore important to figure out which laser energy has to be used for the comparison between the nonresonant theory and the experiment in order to study the magnetic excitations only.

The first criterion can be gained from the optical conductivity as, for example, given in Ref. 20: the intensity of the two-triplon peak develops in the same way as the optical conductivity. For the nonresonant regime, both energy of the incident and scattered light should be smaller than the charge-transfer gap (Sr14: $\Delta_{T=10\text{ K}} \sim 2.1$ eV). Thus, we have chosen spectra with laser energies $\omega_{\text{exc}} = 1.92$ eV in the case of Sr14 and $\omega_{\text{exc}} = 1.95$ eV for Sr123. Luckily, the value of the optical conductivity is about $100 \Omega^{-1} \text{ cm}^{-1}$ in the subgap regime²⁰ at $\omega = \omega_{\text{exc}} - E_{2\text{T}} \sim 1.5$ eV (which is one to two orders of magnitude larger than for the 2D cuprates⁷²), yielding a nonvanishing intensity of the two-triplon peak. Here $E_{2\text{T}}$ denotes the energy of the two-triplon peak.

The second criterion arises from the polarization dependence of the two-triplon peak. Depending on the laser energy used, one can observe a drastic difference in the line shape between the two polarizations.^{19,20} Although the difference in the line shapes is large for $\omega_{\text{exc}} > 2.1$ eV, it does almost vanish in the case of $\omega_{\text{exc}} < 2.0$ eV.²⁰ This fits very well to the weak polarization dependence of the purely magnetic response, as described by Eqs. (3): for $x_{\text{cyc}} = 0.0$, the Raman line shape is identical in the rung and the leg polarization. Small deviations $x_{\text{cyc}} = 0.2$ as relevant for the description of Sr123 and Sr14 produce small deviations with respect to the symmetry between the rung and leg polarization of the ladder. These deviations cannot account for the drastic change

between the two polarizations as observed for $\omega_{\text{exc}} > 2.1$ eV.^{19,20} We therefore conclude that the spectra $\omega_{\text{exc}} < 2.0$ eV are the best choice in order to compare to a purely magnetic, nonresonant theory.

Now we discuss the dependence of the width of the two-triplon peak on the parameters x and x_{cyc} . In Fig. 2, the full width at half maximum (FWHM) of the two-triplon peak is shown. The overall uncertainty shown as error bars in Fig. 2 of the extrapolated two-triplon FWHM was determined by comparing to DMRG data.⁷³

Let us first consider the case $x_{\text{cyc}} = 0.0$. Here the two-triplon width should be identical in both polarizations. It can be clearly seen that the numerically obtained results reflect this property rather well, indicating that the uncertainties in the extrapolation are small concerning the matrix elements. There is a strong dependence of the FWHM of the two-triplon peak on the parameter x . The peak sharpens significantly when the ratio x of the magnetic Heisenberg exchanges increases (four times from $x=1$ to $x=1.5$). In the case of $x_{\text{cyc}} \neq 0$, the width depends on the polarization. In general, the width in (xx) polarization is larger than in (yy) polarization. For fixed x the FWHM changes at maximum by a factor of two when varying x_{cyc} from 0 to 0.2.

In Figs. 3(a)–3(d), the experimental Raman response of Sr123 and Sr14 is shown for (xx) and (yy) polarization (red-black and cyan-gray curves). The spectra of Sr123 were taken in the same way as described in Ref. 19. The data of Sr14 has been made available by Gozar *et al.*²⁰ In addition, theoretically obtained two-triplon contributions are displayed (orange-gray and blue-black). Experimentally, the width of the two-triplon peak of both materials is almost identical ($\sim 150 \text{ cm}^{-1}$). Only the position of the two-triplon peak is different ($\sim 3140 \text{ cm}^{-1}$ for Sr123 and $\sim 3000 \text{ cm}^{-1}$ for Sr14), which is a result of the slightly different Madelung potentials of both compounds.

For modeling the Raman response, we assume $x_{\text{cyc}} = 0.2$ for both compounds. This order of magnitude was previously obtained for cuprate ladders by inelastic neutron scattering,^{57,58} by infrared absorption,^{27,28} Raman response,^{19,32} and theoretical works deriving extended low-energy Heisenberg models.^{35,74} In order to account for the FWHM and the two-triplon peak position, we determine $x = 1.5$ and global energy scales $J_{\perp} = 1130 \text{ cm}^{-1}$ for Sr123 and $J_{\perp} = 1080 \text{ cm}^{-1}$ for Sr14. It was previously argued that in Sr14, a charge order of the chain subsystem modulates the magnetic exchange in the ladders.³² This opens a gap in the Raman response that has a large effect on the two-triplon peak for the parameters $x = 1.2$ and $x_{\text{cyc}} = 0.2$, which are appropriate for La6Ca8. However, the effect is small for larger x values because the induced gap opens well above the two-triplon peak at $\sim 3600 \text{ cm}^{-1}$. The set of parameters used above for Sr123 and Sr14 describes quantitatively well the Raman response as shown in Table I and Figs. 3(a)–3(d). Especially both polarizations for each material can be modeled using only one set of parameters J_{\perp} , x , and x_{cyc} . The smaller FWHM of Sr123 and Sr14 compared to La6Ca8^{23,32} can be directly explained by their larger x values (see Fig. 2). The coupling constants of Sr14 are in good agreement with those obtained by IR absorption measurements.⁷⁵ Additionally, our set of parameters yields a spin gap of 290 cm^{-1} for Sr123

and 280 cm^{-1} for Sr14 using the underlying one-triplon dispersion. The latter value is consistent with the spin gap measured by inelastic neutron scattering.⁷⁶

V. CUPRATE PLANES

In this section we calculate the Raman response for the undoped two-dimensional cuprate compounds using a toy model consisting of two uncoupled two-leg ladders (see Fig. 4). This is motivated by the fact that the building blocks of ladders and planes are edge-sharing Cu_4 plaquettes. We expect that the Raman response is dominated by short-range and high-energy excitations, yielding a certain similarity between ladders and planes. Indeed, the positions of the two-magnon peak in the 2D cuprates and the two-triplon peak in the cuprate ladders are found at almost the same frequency $\sim 3000 \text{ cm}^{-1}$, but the FWHM of the two-dimensional compounds is a factor of 2–6 larger. We have shown in Sec. IV that the FWHM of the two-triplon peak in the cuprate ladder compounds strongly varies with x . We therefore conjecture that the larger FWHM of the two-dimensional cuprates originates from the isotropic coupling $x=1$. There will, of course, be deviations at small energies resulting from the differences between a gapped two-leg ladder and the gapless excitations in the two-dimensional compounds. Clearly, a magnon description would be the proper starting point to treat the long-range-ordered antiferromagnetic state. We think, however, that a triplon picture (which includes the interactions on the quantitative level) can give a good description of the Raman response. A similar treatment in terms of gapped quasiparticles already led to an improved agreement between theory and experiments.^{78,79}

In the following we will show how to deduce the A_{1g} and B_{1g} Raman spectra of the square lattice from those of the two-leg ladder. Clearly, one should use $x=1$ because the square lattice is isotropic ($J=J_{\parallel}=J_{\perp}$). Starting from the Fleury-Loudon operator, the observables $\mathcal{O}^{B_{1g}}$ ($\mathcal{O}^{A_{1g}}$) for magnetic light scattering in B_{1g} (A_{1g}) polarization read in leading order for the two-dimensional square lattice^{62,63}

$$\mathcal{O}^{B_{1g}} = A_{0,B_{1g}} \left(\sum_{\langle ij \rangle, x} \mathbf{S}_i \mathbf{S}_j - \sum_{\langle ij \rangle, y} \mathbf{S}_i \mathbf{S}_j \right) \quad (4a)$$

$$\mathcal{O}^{A_{1g}} = A_{0,A_{1g}} \left(\sum_{\langle ij \rangle, x} \mathbf{S}_i \mathbf{S}_j + \sum_{\langle ij \rangle, y} \mathbf{S}_i \mathbf{S}_j \right). \quad (4b)$$

Here $\langle ij \rangle, x$ ($\langle ij \rangle, y$) denotes a summation over nearest neighbors in the x direction (y direction). The parameters $A_{0,B_{1g}}$ and $A_{0,A_{1g}}$ depend on the underlying microscopic model and are, in general, not equal.⁶³ We approximate the two-dimensional square lattice by a sum of two uncoupled two-leg ladders, one oriented in x direction, the other in y direction. The situation is sketched in Fig. 4. The summation over both ladder orientations will restore the square lattice symmetries. Comparing Eq. (4) with Eq. (3) one readily deduces the following relations:

$$\mathcal{O}^{B_{1g}} \propto (\mathcal{O}^{\text{leg}} - \mathcal{O}^{\text{rung}}) \quad (5a)$$

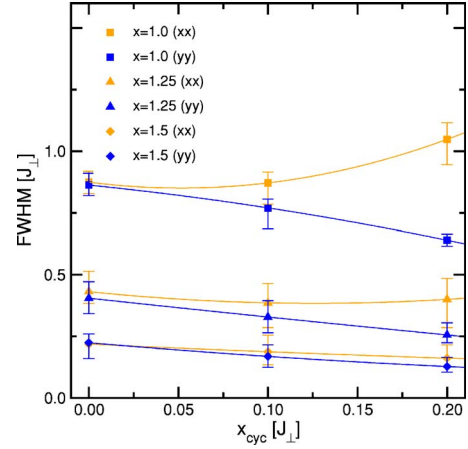


FIG. 2. (Color online) The FWHM of the two-triplon peak for $x := J_{\parallel}/J_{\perp} = 1$ (squares), $x = 1.25$ (triangles) and $x = 1.5$ (diamonds) as a function of the strength of the four-spin interactions $x_{\text{cyc}} := J_{\text{cyc}}/J_{\perp}$. The orange (gray) symbols denote (xx) polarization and the blue (black) symbols (yy) polarization. The solid lines are a guide to the eye obtained by spline interpolation.

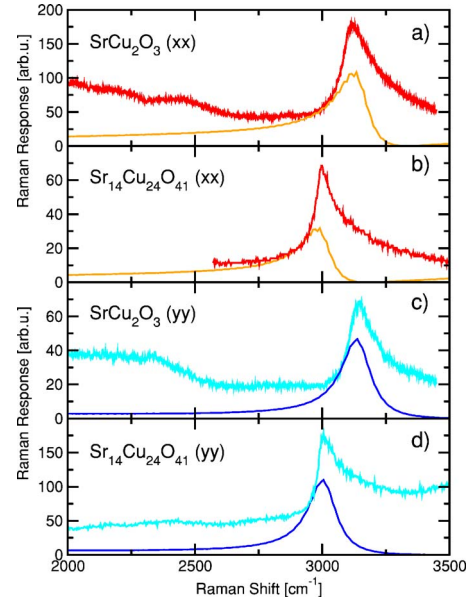


FIG. 3. (Color online) Comparison of the magnetic Raman response of Sr123 ($T=25 \text{ K}$) and Sr14 ($T=5 \text{ K}$) with the theoretically obtained two-triplon contribution. The data of Sr14 have been provided by Gozar *et al.*²⁰ (a) The red (black) curve denotes the (xx) polarization ($x \parallel b$) of Sr123 with a laser excitation energy $\omega_{\text{exc}} = 1.95 \text{ eV}$. The orange (gray) curve displays the theoretical two-triplon contribution with $x=1.5$, $x_{\text{cyc}}=0.2$, and $J_{\perp}=1130 \text{ cm}^{-1}$. (b) The red (black) curve denotes the (xx) polarization ($x \parallel a$) of Sr14 with a laser excitation energy $\omega_{\text{exc}} = 1.92 \text{ eV}$. The orange (gray) curve displays the theoretical two-triplon contribution with $x=1.5$, $x_{\text{cyc}}=0.2$, and $J_{\perp}=1080 \text{ cm}^{-1}$. (c) (yy) polarization ($y \parallel a$) for Sr123; identical parameters as in (a). The cyan (gray) curve displays the experimental data, and the blue (black) curve the theoretical two-triplon contribution. (d) (yy) polarization ($y \parallel c$) for Sr14; identical parameters as in (b) and the same colors as in (c).

TABLE I. Comparison of the two-triplon peak between experimental data of different cuprate ladder and plane compounds and the theoretical results.

Material	Experiment				Theory (CUT)			
	Peak (cm ⁻¹)	FWHM ^a (cm ⁻¹)	ω_{exc} (eV)	Ref.	x	x_{cyc}	J_{\perp} (cm ⁻¹)	FWHM (cm ⁻¹)
SrCu ₂ O ₃ (xx)	3120	150–220	1.96	this work	1.5	0.2	1130	180
SrCu ₂ O ₃ (yy)	3150	120–180	1.96	this work	1.5	0.2	1130	140
Sr ₁₄ Cu ₂₄ O ₄₁ (xx)	3000	100–160	1.92	20	1.5	0.2	1080	180
Sr ₁₄ Cu ₂₄ O ₄₁ (yy)	3000	120 ^b	1.92	20	1.5	0.2	1080	140
La ₆ Ca ₈ Cu ₂₄ O ₄₁ (xx)	3010	550 ^b	2.41	23 and 32	1.2	0.2	1130	580
La ₆ Ca ₈ Cu ₂₄ O ₄₁ (yy)	2950	350 ^b	2.41	23 and 32	1.2	0.2	1130	350
Sr ₂ CuO ₂ Cl ₂	2950	800–1100	2.73	5	1.0	0.2	1190	1000
YBa ₂ Cu ₃ O _{6+δ}	2750	1000–1150	2.71	6	1.0	0.2	1110	940
La ₂ CuO ₄	3170	950–1150	2.71	6	1.0	0.2	1280	1080
Nd ₂ CuO ₄	2930	900–1050	2.71	6	1.0	0.2	1190	1000

^aLower limit of exp. FWHM: linear background subtracted from data. Upper limit: no background corrections.

^bExp. FWHM: linear background subtracted from data because background exceeds almost the two-triplon peak heights.

$$\mathcal{O}^{A_{1g}} \propto (\mathcal{O}^{\text{leg}} + \mathcal{O}^{\text{rung}}) \quad (5b)$$

between the relevant observables in the two-leg ladder and the two-dimensional square lattice. Note that for $x_{\text{cyc}}=0$, the Raman response in the A_{1g} polarization vanishes because of the property $\mathcal{O}^{\text{leg}}|0\rangle = -\mathcal{O}^{\text{rung}}|0\rangle$.²⁶ The latter point is consistent with earlier treatments of the two-dimensional Raman response. But for a finite strength of the four-spin interactions x_{cyc} , also the A_{1g} polarization is finite.^{43,46}

The theoretical two-triplon contribution of the B_{1g} and the A_{1g} polarization is shown in Fig. 5(a) and 5(b). The parameters used are an isotropic coupling $x=1$ and a strength of the four-spin interactions $x_{\text{cyc}}=0.0$, $x_{\text{cyc}}=0.1$, and $x_{\text{cyc}}=0.2$.

The B_{1g} polarization displays a symmetric two-triplon peak, which is dominating the Raman response. The four-spin interactions shift the whole spectrum to lower energies and decrease the total intensity. The FWHM of the two-triplon peak is approximately given by the average width of the two-triplon peaks of an isolated two-leg ladder in rung and in leg polarization. Thus, the width is nearly independent of the value of x_{cyc} .

The A_{1g} polarization is almost zero for vanishing x_{cyc} . This again reflects the accurate extrapolation of the matrix

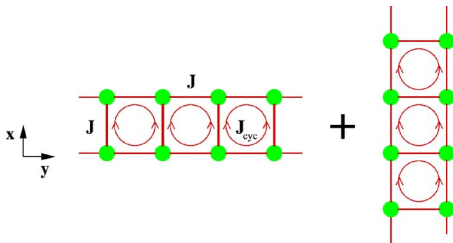


FIG. 4. (Color online) Sketch of two uncoupled spin ladders. Here one ladder is oriented in y direction and the other in x direction. We approximate the two-dimensional square lattice by the sum of these two uncoupled orthogonal ladders.

elements. For nonzero x_{cyc} , a finite A_{1g} contribution is realized. The differences in the line shape between A_{1g} and B_{1g} are a pure effect of different matrix elements. Compared to the two-triplon peak in the B_{1g} polarization, the A_{1g} polarization displays a two peak structure where the second peak is sharper and at higher energies.

In the following we will compare the theoretical two-triplon contribution to the Raman response with low-temperature experimental data on $R_2\text{CuO}_4$ ($\omega_{\text{exc}}=2.71$ eV),⁶ $\text{Sr}_2\text{CuO}_2\text{Cl}_2$ ($\omega_{\text{exc}}=2.73$ eV),⁵ and $\text{YBa}_2\text{Cu}_3\text{O}_{6+\delta}$ ($\omega_{\text{exc}}=2.71$ eV)⁶ taken from the literature.

As discussed in Sec. IV, the laser energy used for the experiment is a crucial issue. Analogous to the ladders, one should use spectra of cuprate planes measured with laser energies below the charge gap for comparing to the purely

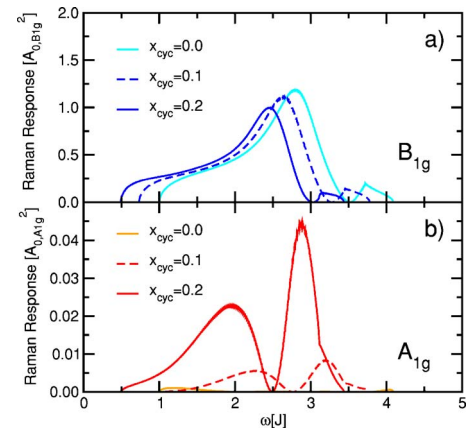


FIG. 5. (Color online) Two-triplon Raman response of the 2D square lattice for $x=1$. (a) B_{1g} polarization for $x_{\text{cyc}}=0.0$ [cyan (gray)], $x_{\text{cyc}}=0.1$ (dashed) and $x_{\text{cyc}}=0.2$ [blue (black)]. (b) A_{1g} polarization for $x_{\text{cyc}}=0.0$ [orange (gray)], $x_{\text{cyc}}=0.1$ (dashed) and $x_{\text{cyc}}=0.2$ [red (black)]. Note the different scales for the Raman response in A_{1g} and B_{1g} spectra.

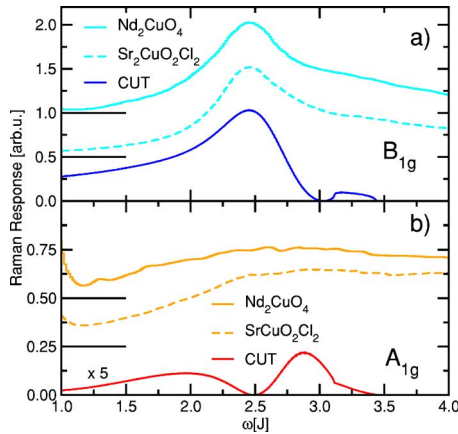


FIG. 6. (Color online) Comparison of the two-triplon Raman response to the two-magnon Raman line shape of Nd_2CuO_4 ($\omega_{\text{exc}} = 2.71$ eV, $T = 30$ K) and $\text{Sr}_2\text{CuO}_2\text{Cl}_2$ ($\omega_{\text{exc}} = 2.73$ eV, $T = 5$ K). The Raman data of Nd_2CuO_4 and $\text{Sr}_2\text{CuO}_2\text{Cl}_2$ are reproduced from Refs. 6 and 5. The experimental curves are smoothed and their zero position is shifted horizontally as indicated by the black horizontal lines. (a) B_{1g} polarization: The blue (black) curve denotes the two-triplon contribution with $x=1$ and $x_{\text{cyc}}=0.2$. The global energy scale J is chosen such that experimental two-magnon and the theoretical two-triplon peak merge. This yields $J=1190$ cm^{-1} for Nd_2CuO_4 [cyan(grey)] and $\text{Sr}_2\text{CuO}_2\text{Cl}_2$ (dashed). (b) A_{1g} polarization [theory: red (black); experiment: orange (grey)]: Same notations as in (a). Note that the *same* magnetic exchange couplings J are used. The A_{1g} -CUT is multiplied by a factor of 5 in comparison to the curve in Fig. 5.

magnetic theoretical response. But it turns out that the optical conductivity is rather low (≤ 10 $\Omega^{-1} \text{cm}^{-1}$) below the charge gap Δ , which results in a vanishing intensity of the two-magnon peak.⁵ An analogous choice of the laser energies below the charge gap, as discussed for the cuprate ladders is not possible. Therefore, we used data measured with laser energies $\omega_{\text{exc}} = 2.7$ eV $> \Delta$. At the energy $\omega_{\text{exc}} = 2.7$ eV, the optical conductivity is quite smooth and $\omega_{\text{exc}} \neq \Delta \approx (1.7-2.0)$ eV.^{5,72,77} Simultaneously, $\omega_{\text{exc}} = 2.7$ eV coincides with the triple resonance at $\omega_{\text{res}} \approx \Delta + 8J$. The triple resonance theory predicts two peaks in the Raman response at about $2.8J$ and $4J$. The relative intensity of both peaks depends on the laser energy. The second peak is strongly suppressed at ω_{res} . In that sense this laser energy can be assigned to be closest to the non-resonant regime.⁵²⁻⁵⁴

In Fig. 6, experimental data and theoretical contributions using $x=1$ and $x_{\text{cyc}}=0.2$ are shown for both polarizations. Frequencies are measured in units of J . We first discuss the B_{1g} polarization in Fig. 6(a). We have chosen the global energy scale J for all experimental curves such that the positions of the experimental two-magnon and the theoretical two-triplon peaks match. This yields quantitatively reasonable values for these compounds. In addition, we find quantitative agreement between the experimental FWHM and the theoretical FWHM of the two-triplon peak. The values of J and the FWHM are listed in Table I for all compounds. Note that the FWHM for $x=1$ is larger than for the anisotropic case $x > 1$ as discussed for the ladder compounds.

Clearly, there are also deviations between theory and experiment. As expected, the low-energy spectral weight in the

theoretical line shape is larger compared to the experimental curves. This is definitely a consequence of approximating the two-dimensional square lattice with quasi-one-dimensional models. There is also spectral weight missing at higher energies above the two-triplon peak. Possible explanations will be described below.

The results for the A_{1g} polarization [shown in Fig. 6(b)] are explained next. We used the *same* global energy scales J for the experimental curves as determined from the B_{1g} polarization above. In order to reproduce the maximum intensity of the experiment, we multiplied the theoretical curve from Fig. 5(b) by a factor 5. This implies that the microscopic parameters $A_{0,B_{1g}}$ and $A_{0,A_{1g}}$ are anisotropic. A possible reason for this anisotropy could be the restriction to the Fleury-Loudon observable. An extension of this observable to higher orders in t/U (four-spin and next-nearest neighbor two-spin terms) gives additional contributions to $\mathcal{O}^{B_{1g}}$ and $\mathcal{O}^{A_{1g}}$.⁶³ The relevance of these contributions has not been analyzed.

In the experiment a broad hump is measured. We find it very promising that the theoretical contribution displays the dominant spectral weight just for these energies. However, the line shape cannot be resolved completely because the dip in the theoretical curve is not observed in the experiment. It originates from neglecting the finite lifetime effects, which are already present in the description of the isolated two-leg ladder^{32,70} being the building block of our square-lattice toy model. We conclude that at least a part of the experimental A_{1g} polarization originates from the finite four-spin interactions. For $x_{\text{cyc}}=0$, there is no purely magnetic contribution to the Raman response for this polarization. A finite A_{1g} Raman response can be regarded as an evidence for the presence of sizable four-spin interactions. This follows entirely from symmetry arguments and holds true for the full two-dimensional model. At higher energies, spectral weight is missing in the theoretical contribution in an analogous fashion as in the B_{1g} polarization.

VI. HIGH-ENERGY SPECTRAL WEIGHT

As shown in Secs. IV and V, the CUT cannot account for the missing high-energy spectral weight when comparing to the Raman experiments. Also other theories proposed previously like calculations based on spin-waves,^{41,42} paramagnons,⁷⁸ Jordan-Wigner fermions,⁷⁹ and numerical studies^{26,44,55,56} were faced with the same problem. Extended theories, including (i) multiparticle contributions, (ii) spin-phonon coupling, (iii) two-magnon or two-triplon plus phonon absorption, and (iv) triple resonance are necessary in order to describe the high-energy spectral weight.

Most of the publications deal with the two-dimensional compounds. Here we will try to review these ideas and reexamine them in the light of our results. Especially, the quantitative results for the cuprate ladders can give insight in this discussion.

A. Multiparticle contributions

One open problem is the role of multiparticle contributions to the Raman response, i.e., the four-magnon contribu-

tion in the case of the square lattice and the four-triplon contribution in the case of the two-leg ladder. At this stage no quantitative calculations are available. But it is known that the multitriplon spectral weights are sizable for the two-leg ladder.^{26,70} The main effect of the four-spin interaction on the high-energy spectral weight is a small shift from the two-triplon to the multitriplon channels.⁷⁰ But this shift is not sufficient to account for the high-energy spectral weight as observed in experiments. This was also found in treatments for the two-dimensional square lattice.^{18,43,45} However, the complete magnetic infrared absorption spectrum (including the high-energy part) of La6Ca8 can be described quantitatively by including multiparticle contributions.^{27,28} Here x_{cyc} does not play the dominant role for the high-energy spectral weight.⁸⁰

It is therefore plausible that these contributions give a noticeable effect also on the high-energy Raman response. There are also indications that the spectral weight cannot be fully explained in this way. For example, the four-magnon spectral weight was shown to be negligible for the 2D square lattice.⁴² But the magnon-magnon interaction, which was not treated in this calculation, could enhance the high-energy spectral weight. Also quantum Monte Carlo calculations, which include all magnon contributions for the two-dimensional Heisenberg model, seem to explain only a part of the high-energy spectral weight.⁴⁴ But finite-size effects and inaccuracies of the analytical continuation can lead to uncertainties in determining the high-energy spectral weight.

B. Spin-phonon coupling

The latter observations suggest that additional degrees of freedom are important. It was argued by several authors that the coupling to phonons produces a large amount of spectral weight above the two-triplon peak.^{4,46,48-51} In one approach the spin-phonon coupling modulates the magnetic exchange couplings with a Gaussian distribution. Another approach introduces a finite spin-wave damping induced by the spin-phonon coupling. Both scenarios produce a significantly broadened and asymmetric two-magnon peak as observed in experiments.^{50,51}

Nevertheless, the consistency of a spin-phonon coupling as suggested above with experiments is not clear. The magnitude of this coupling has to be unrealistically large in order to describe infrared absorption data.¹⁷ Additionally, it was pointed out by Freitas and Singh⁸¹ that the temperature-dependent correlation length and the spin dynamics, which agree well with purely magnetic models, does not leave room for such a coupling.^{82,83}

There are no investigations of the role of spin-phonon couplings for the case of the cuprate ladder systems. But the FWHM of the two-triplon peak can be quantitatively understood within a purely magnetic model as shown in Sec. IV. Thus, we conclude that the spin-phonon coupling is not strong in the case of the cuprate ladder compounds. Such a coupling leads to a broad two-triplon peak in the same way as for the two-dimensional case. This is a contradiction when considering the Raman response and the infrared absorption of cuprate ladders, simultaneously: on the one hand, one

needs a larger anisotropy between leg and rung coupling (larger x) in order to sharpen the two-triplon peak in the Raman response again (see Fig. 2); but on the other hand, one cannot explain the infrared absorption with a substantially increased x .^{27,75} A strong spin-phonon coupling is, therefore, in contradiction with the results obtained for cuprate ladders. This can be also seen as an indication that the same holds true for the two-dimensional compounds.⁴

C. Two-magnon or two-triplon plus phonon absorption

A third alternative explaining the high-energy spectral weight uses phonons as possible momentum sinks. Here a strong spin-phonon coupling is not necessary. The idea is based on the work of Lorenzana and Sawatzky for infrared absorption.^{18,84,85} It is well accepted in the case of infrared absorption measurements on cuprate ladders^{27,80} and planes^{17,18} that the dominant processes are magnetic excitations, which are assisted by phonons. It was realized by Freitas and Singh that similar processes could be important also for the Raman response in cuprate planes.⁸¹ In an analogous fashion a two-triplon plus (Raman active) phonon process for the Raman response in cuprate ladders could be important. It can be used to transfer spectral weight above the two-triplon peak leading to an asymmetric line shape. It is a difficult task to determine the relative strength of this process compared to the usual two-triplon scattering.

D. Triple resonance

Additionally, the triple resonance was proposed to account for the high-energy spectral weight in the two-dimensional compounds.^{5,52-54} As already stated in Sec. V, the experimental spectra of the planes are taken in the resonant regime. It is known that the triple resonance scenario yields an additional peak above the two-magnon peak. Its intensity depends significantly on the energy of the incident light in accordance with experiments.⁵ In principle, the same effect is also present in ladder compounds. But for the laser energy $\omega_{\text{exc}} = 1.92 \text{ eV} < \Delta$ considered for Sr123 and Sr14, the triple resonance condition is not fulfilled.

Because of the simplified model used for the 2D system, no conclusion about the high-energy weight can be drawn from our results. Because a large spin-phonon coupling and the triple resonance can be ruled out for the cuprate ladder systems, the observed high-energy spectral weight in the cuprate ladder compounds has to be explained most probably by the multitriplon or two-triplon plus phonon contributions.

VII. CONCLUSION

The first part of this work deals with the theoretical understanding of nonresonant magnetic Raman scattering on cuprate two-leg ladder compounds, namely, Sr123, Sr14, and La6Ca8. Therefore, we applied a triplon-conserving CUT on a microscopic spin-model which includes Heisenberg couplings and additional four-spin interactions. We studied the two-triplon contribution to the nonresonant magnetic Raman

response. The dominating feature of the two-triplon contribution is the two-triplon peak, which has a characteristic FWHM depending on the model parameters x and x_{cyc} . We carefully chose the experimental data closest to the non-resonant regime and compared them with our theory.

The key observation we found is that the sharpness of the two-triplon peak in Sr123 and Sr14 in comparison to La6Ca8 can be explained by the stronger anisotropy of the magnetic exchange along the rungs and legs of the ladder. Indeed, the two-triplon peak width depends strongly on the parameter x . Both materials can be modeled with the parameters $x \approx 1.5$ and $x_{\text{cyc}} \approx 0.2$, but different global energy scales $J_{\perp} \approx 1130 \text{ cm}^{-1}$ for Sr123 and $J_{\perp} \approx 1080 \text{ cm}^{-1}$ for Sr14. The parameters for Sr14 are in good agreement with infrared absorption^{27,75} and inelastic neutron scattering⁷⁶ experiments. We conclude that the dominating two-triplon peak of the magnetic Raman response in cuprate ladders can be consistently explained within the microscopic model. The presence of a four-spin interaction of the order of $0.2J_{\perp}$ can be viewed as a settled issue.

In the second part of this paper we used the results found for the two-leg ladder to describe the magnetic Raman response of the undoped two-dimensional cuprate compounds in B_{1g} and A_{1g} polarization. The contribution to the A_{1g} polarization is only allowed for finite four-spin interactions due to symmetry reasons. We use an isotropic coupling $x=1$ and $x_{\text{cyc}}=0.2$ for the comparison with the experimental data. Convincingly, we find quantitative agreement for the two-triplon peak position *and* the two-triplon peak width for several compounds. Additionally, a sizable spectral weight is found in the A_{1g} polarization consistent with experiments.

We conclude that the processes dominating the magnetic Raman response are short ranged.

The last part deals with the missing high-energy spectral weight above the dominating two-triplon peak for the case of cuprate ladders and planes. We review possible sources of this spectral weight, such as multiparticle contributions, the role of spin-phonon coupling, a two-triplon plus phonon process, and the triple resonance to the magnetic Raman response. We deduced from our results that the high-energy spectral weight cannot be explained with realistic values for the spin-phonon coupling.

In summary, our calculations lead to an unified understanding of the magnetic Raman response in cuprate ladder compounds within a purely magnetic model. A strong spin-phonon coupling can be excluded for these materials. Additionally, we obtained a convincing quantitative description of the dominating two-magnon peak in the Raman response of cuprate planes using a toy model consisting of two uncoupled two-leg ladders. This suggests that the short-range triplon excitations might be an alternative starting point for the description of the two-dimensional cuprate compounds.

ACKNOWLEDGMENT

We gratefully acknowledge G. S. Uhrig, M. Grüninger, A. Gozar, A. Reischl, and S. Jandl for very helpful discussions. We thank A. Gozar for the kind provision of experimental data on Sr14. This work is supported by the DFG in SFB 608.

*Electronic address: ks@thp.uni-koeln.de

¹J. Orenstein and A. J. Millis, *Science* **288**, 468 (2000).

²S. Sachdev, *Science* **288**, 475 (2000).

³P. W. Anderson, *Science* **288**, 480 (2000).

⁴P. Knoll, C. Thomsen, M. Cardona, and P. Murugaraj, *Phys. Rev. B* **42**, 4842 (1990).

⁵G. Blumberg, P. Abbamonte, M. V. Klein, W. C. Lee, D. M. Ginsberg, L. L. Miller, A. Zibold, *Phys. Rev. B* **53**, R11930 (1996).

⁶S. Sugai, M. Sato, T. Kobayashi, J. Akimitsu, T. Ito, H. Takagi, S. Uchida, S. Hosoya, T. Kajitani, and T. Fukuda, *Phys. Rev. B* **42**, R1045 (1990).

⁷P. E. Sulewski, P. A. Fleury, K. B. Lyons, S.-W. Cheong, and Z. Fisk, *Phys. Rev. B* **41**, 225 (1990).

⁸P. E. Sulewski, P. A. Fleury, K. B. Lyons, and S.-W. Cheong, *Phys. Rev. Lett.* **67**, 3864 (1991).

⁹M. Yoshida, S. Tajima, N. Koshizuka, S. Tanaka, S. Uchida, and T. Itoh, *Phys. Rev. B* **46**, 6505 (1992).

¹⁰E. Manousakis, *Rev. Mod. Phys.* **63**, 1 (1991).

¹¹M. A. Kastner, R. J. Birgeneau, G. Shirane, and Y. Endoh, *Rev. Mod. Phys.* **70**, 897 (1998).

¹²S. J. Clarke, A. Harrison, T. E. Mason, and D. Visser, *Solid State Commun.* **112**, 561 (1999).

¹³S. M. Hayden, G. Aeppli, R. Osborn, A. D. Taylor, T. G. Perring,

S.-W. Cheong, and Z. Fisk, *Phys. Rev. Lett.* **67**, 3622 (1991).

¹⁴R. Coldea, S. M. Hayden, G. Aeppli, T. G. Perring, C. D. Frost, T. E. Mason, S.-W. Cheong, and Z. Fisk, *Phys. Rev. Lett.* **86**, 5377 (2001).

¹⁵J. D. Perkins, J. M. Graybeal, M. A. Kastner, R. J. Birgeneau, J. P. Falck, and M. Greven, *Phys. Rev. Lett.* **71**, 1621 (1993).

¹⁶J. D. Perkins, R. J. Birgeneau, J. M. Graybeal, M. A. Kastner, and D. S. Kleinberg, *Phys. Rev. B* **58**, 9390 (1998).

¹⁷M. Grüninger, D. van der Marel, A. Damascelli, A. Erb, T. Nunner, and T. Kopp, *Phys. Rev. B* **62**, 12422 (2000).

¹⁸J. Lorenzana, J. Eroles, and S. Sorella, *Phys. Rev. Lett.* **83**, 5122 (1999).

¹⁹A. Gößling, U. Kuhlmann, C. Thomsen, A. Löffert, C. Gross, and W. Assmus, *Phys. Rev. B* **67**, 052403 (2003).

²⁰A. Gozar, G. Blumberg, B. S. Dennis, B. S. Shastry, N. Motoyama, H. Eisaki, and S. Uchida, *Phys. Rev. Lett.* **87**, 197202 (2001).

²¹E. Dagotto and T. M. Rice, *Science* **271**, 618 (1996).

²²Z. V. Popović, M. J. Konstantinović, V. A. Ivanov, O. P. Khuong, R. Gajić, A. Vietkin, and V. V. Moshchalkov, *Phys. Rev. B* **62**, 4963 (2000).

²³S. Sugai and M. Suzuki, *Phys. Status Solidi B* **215**, 653 (1999).

²⁴K. P. Schmidt and G. S. Uhrig, *Phys. Rev. Lett.* **90**, 227204 (2003).

- ²⁵C. Knetter, K. P. Schmidt, M. Grüninger, and G. S. Uhrig, Phys. Rev. Lett. **87**, 167204 (2001).
- ²⁶K. P. Schmidt, C. Knetter, and G. S. Uhrig, Europhys. Lett. **56**, 877 (2001).
- ²⁷T. S. Nunner, P. Brune, T. Kopp, M. Windt, and M. Grüninger, Phys. Rev. B **66**, 180404(R) (2002).
- ²⁸M. Grueninger, M. Windt, E. Benckiser, T. S. Nunner, K. P. Schmidt, G. S. Uhrig, and T. Kopp, Adv. Solid State Phys. **43**, 95 (2003).
- ²⁹W. Zheng, C. J. Hamer, and R. R. P. Singh, Phys. Rev. Lett. **91**, 037206 (2003).
- ³⁰K. P. Schmidt, C. Knetter, and G. S. Uhrig, Phys. Rev. B **69**, 104417 (2004).
- ³¹S. Trebst, H. Monien, C. J. Hamer, Z. Weihong, and R. R. P. Singh, Phys. Rev. Lett. **85**, 4373 (2000).
- ³²K. P. Schmidt, C. Knetter, M. Grüninger, and G. S. Uhrig, Phys. Rev. Lett. **90**, 167201 (2003).
- ³³S. Brehmer, H.-J. Mikeska, M. Müller, N. Nagaosa, and S. Uchida, Phys. Rev. B **60**, 329 (1999).
- ³⁴E. Müller-Hartmann and A. Reischl, Eur. Phys. J. B **28**, 173 (2002).
- ³⁵Y. Mizuno, T. Tohyama, and S. Maekawa, J. Phys. Soc. Jpn. **66**, 397 (1997).
- ³⁶H. J. Schmidt and Y. Kuramoto, Physica C **167**, 263 (1990).
- ³⁷M. Takahashi, J. Phys. C **10**, 1289 (1977).
- ³⁸A. H. MacDonald, S. M. Girvin, D. Yoshioka, Phys. Rev. B **41**, 2565 (1990).
- ³⁹M. Roger and J. M. Delrieu, Phys. Rev. B **39**, 2299 (1989).
- ⁴⁰A. Reischl, E. Müller-Hartmann, G. S. Uhrig, Phys. Rev. B **70**, 245124 (2004).
- ⁴¹R. R. P. Singh, P. A. Fleury, K. B. Lyons, and P. E. Sulewski, Phys. Rev. Lett. **62**, 2736 (1989).
- ⁴²C. M. Canali and S. M. Girvin, Phys. Rev. B **45**, 7127 (1992).
- ⁴³Y. Honda, Y. Kuramoto, and T. Watanabe, Phys. Rev. B **47**, 11329 (1993).
- ⁴⁴A. W. Sandvik, S. Capponi, D. Poilblanc, and E. Dagotto, Phys. Rev. B **57**, 8478 (1998).
- ⁴⁵A. A. Katanin and A. P. Kampf, Phys. Rev. B **67**, 100404(R) (2003).
- ⁴⁶J. Erole, C. D. Batista, S. B. Bacci, and E. R. Gagliano, Phys. Rev. B **59**, 1468 (1999).
- ⁴⁷M. J. Reilly and A. G. Rojo, Phys. Rev. B **53**, 6429 (1996).
- ⁴⁸D. U. Saenger, Phys. Rev. B **52**, 1025 (1995).
- ⁴⁹W. H. Weber and G. W. Ford, Phys. Rev. B **40**, 6890 (1989).
- ⁵⁰S. Haas, E. Dagotto, J. Riera, R. Merlin, and F. Nori, J. Appl. Phys. **75**, 6340 (1994).
- ⁵¹F. Nori, R. Merlin, S. Haas, A. W. Sandvik, and E. Dagotto, Phys. Rev. Lett. **75**, 553 (1995).
- ⁵²A. V. Chubukov and D. M. Frenkel, Phys. Rev. Lett. **74**, 3057 (1995).
- ⁵³F. Schönfeld, A. P. Kampf, and E. Müller-Hartmann, Z. Phys. B: Condens. Matter **102**, 25 (1997).
- ⁵⁴D. K. Morr and A. V. Chubukov, Phys. Rev. B **56**, 9134 (1997).
- ⁵⁵C. Jurecka, V. Grützun, A. Friedrich, and W. Brenig, Eur. Phys. J. B **21**, 469 (2001).
- ⁵⁶Y. Natsuma, Y. Watabe, and T. Suzuki, J. Phys. Soc. Jpn. **67**, 3314 (1998).
- ⁵⁷M. Matsuda, K. Katsumata, R. S. Eccleston, S. Brehmer, and H. J. Mikeska, J. Appl. Phys. **87**, 6271 (2000).
- ⁵⁸M. Matsuda, K. Katsumata, R. S. Eccleston, S. Brehmer, and H.-J. Mikeska, Phys. Rev. B **62**, 8903 (2000).
- ⁵⁹Sr14 has intrinsically six holes per unit cell, but it is believed that the majority of the holes are located in the chain subsystem (see Ref. 60).
- ⁶⁰N. Nücker, M. Merz, C. A. Kuntscher, S. Gerhold, S. Schuppler, R. Neudert, M. S. Golden, J. Fink, D. Schild, S. Stadler, V. Chakarian, J. Freeland, Y. U. Idzerda, K. Conder, M. Uehara, T. Nagata, J. Goto, J. Akimitsu, N. Motoyama, H. Eisaki, S. Uchida, U. Ammerahl, and A. Revcolevschi, Phys. Rev. B **62**, 14384 (2000).
- ⁶¹Neglecting the two-spin exchange terms along the diagonals, our notation $J_{\perp}, J_{\parallel}, J_{\text{cyc}}$ is given in terms of the other notation $J_{\perp}^p, J_{\parallel}^p, J_{\text{cyc}}^p$ using cyclic permutations by $J_{\parallel} = J_{\parallel}^p + \frac{1}{4}J_{\text{cyc}}^p$, $J_{\perp} = J_{\perp}^p + \frac{1}{2}J_{\text{cyc}}^p$, and $J_{\text{cyc}} = J_{\text{cyc}}^p$ (see Ref. 33).
- ⁶²P. A. Fleury and R. Loudon, Phys. Rev. **166**, 514 (1968).
- ⁶³B. S. Shastry and B. I. Shraiman, Phys. Rev. Lett. **65**, 1068 (1990).
- ⁶⁴C. Knetter and G. S. Uhrig, Eur. Phys. J. B **13**, 209 (2000).
- ⁶⁵C. Knetter, K. P. Schmidt, and G. S. Uhrig, J. Phys.: Condens. Matter **36**, 7889 (2003).
- ⁶⁶C. Knetter, K. P. Schmidt, and G. S. Uhrig, Eur. Phys. J. B **36**, 525 (2004).
- ⁶⁷K. P. Schmidt, C. Knetter, and G. S. Uhrig, Acta Phys. Pol. B **34**, 1481 (2003).
- ⁶⁸K. P. Schmidt, H. Monien, and G. S. Uhrig, Phys. Rev. B **67**, 184413 (2003).
- ⁶⁹C. Domb and J. L. Lebowitz, *Phase Transitions and Critical Phenomena*, Academic Press, New York (1989), Vol. 13.
- ⁷⁰K. P. Schmidt, Ph.D. thesis, University of Cologne, 2004.
- ⁷¹A. Löffert, C. Gross, and W. Assmus, J. Cryst. Growth **237**, 796 (2002).
- ⁷²H. S. Choi, Y. S. Lee, T. W. Noh, E. J. Choi, Y. Bang, and Y. J. Kim, Phys. Rev. B **60**, 4646 (1999).
- ⁷³The extrapolation of the matrix elements are relatively accurate. The maximum deviation between the two-triplon widths in both polarizations is $0.03J_{\perp}$ for $x_{\text{cyc}}=0$. The one-triplon hopping elements yield a quantitative one-triplon dispersion when compared to DMRG data (see Ref. 27). So we conclude that the largest extrapolation error is due to the extrapolation of the two-triplon interaction amplitudes. To get an estimate of this error we compared the energy of the $S=0$ two-triplon bound state at finite momentum for $x_{\text{cyc}}=0$ obtained by DMRG to the results of the CUT. Then we changed the two-triplon interaction for the Raman case by the maximum deviation of the bound state energies and calculated the effect on the FWHM of the two-triplon peak. In the end we added $0.03J_{\perp}$ to account for the uncertainty of the matrix elements. The resulting uncertainties are shown as error bars in Fig. 2.
- ⁷⁴C. J. Calzado, C. de Graaf, E. Bordas, R. Caballol, and J.-P. Malrieu, Phys. Rev. B **67**, 132409 (2003).
- ⁷⁵M. Windt, Ph.D. thesis, University of Cologne, 2003.
- ⁷⁶R. S. Eccleston, M. Uehara, J. Akimitsu, H. Eisaki, N. Motoyama, and S.-I. Uchida, Phys. Rev. Lett. **81**, 1702 (1998).
- ⁷⁷D. Salamon, Ran Liu, M. V. Klein, M. A. Karlow, S. L. Cooper, S.-W. Cheong, W. C. Lee, and D. M. Ginsberg, Phys. Rev. B **51**, 6617 (1995).
- ⁷⁸T. C. Hsu, Phys. Rev. B **41**, 11379 (1990).
- ⁷⁹Y. R. Wang, Phys. Rev. B **43**, 13774 (1991).
- ⁸⁰M. Windt, M. Grüninger, T. Nunner, C. Knetter, K. P. Schmidt, G. S. Uhrig, T. Kopp, A. Freimuth, U. Ammerahl, B. Büchner,

- and A. Revcolevschi, Phys. Rev. Lett. **87**, 127002 (2001).
- ⁸¹P. J. Freitas and R. R. P. Singh, Phys. Rev. B **62**, 5525 (2000).
- ⁸²Y. Endoh, K. Yamada, R. J. Birgeneau, D. R. Gabbe, H. P. Jensen, M. A. Kastner, C. J. Peters, P. J. Picone, T. R. Thurston, J. M. Tranquada, G. Shirane, Y. Hidaka, M. Oda, Y. Enomoto, M. Suzuki, and T. Murakami, Phys. Rev. B **37**, 7443 (1988).
- ⁸³S. Chakravarty, B. I. Halperin, and D. R. Nelson, Phys. Rev. B **39**, 2344 (1989) and B. Dabrowski, *ibid.* **49**, R13295 (1994).
- ⁸⁴J. Lorenzana and G. A. Sawatzky, Phys. Rev. Lett. **74**, 1867 (1995).
- ⁸⁵J. Lorenzana and G. A. Sawatzky, Phys. Rev. B **52**, 9576 (1995).